Direction-of-arrival, direction-of-departure and travel-time sensivity kernels obtained through double beamforming in shallow water

Florian Aulanier, Barbara Nicolas, Philippe Roux, Jerome I. Mars

DIRECTION-OF-ARRIVAL, DIRECTION-OF-DEPARTURE AND TRAVEL-TIME SENSITIVITY KERNELS OBTAINED THROUGH DOUBLE BEAMFORMING IN SHALLOW WATER

Florian Aulanier[a], Barbara Nicolas[a], Philippe Roux[b], Jérôme Mars[a].

[a]GIPSA Lab – DIS, 961 rue de la Houille Blanche, BP 46, F-38402 Grenoble CEDEX.
[b]ISTerre, BP 53, 38041 Grenoble CEDEX 9, France.

Florian Aulanier, GIPSA Lab – DIS, 961 rue de la Houille Blanche, BP 46, F-38402 Grenoble CEDEX, phone: +33 4 76 57 43 67 fax: +33 4 76 57 47 90, Florian.Aulanier@gipsa-lab.grenoble-inp.fr

Abstract: *In an oceanic waveguide, local sound speed variations induce acoustic path changes (angles, amplitudes, delays, etc...). Using vertical arrays in emission and reception and double beamforming, it is possible, for each path, to jointly track these changes in term of travel-time (τ), reception angle (θr) and emission angle (θe).*
In order to perform ocean acoustic tomography using these observables, we build sensitivity kernels which link the variations of these observables, measured after double beamforming, to sound speed variations. The construction of these kernels is made in two steps.
A first order Born approximation of the Green's function is firstly used to derive the Helmholtz equation and obtain the link between the variations of the sound speed distribution and the variations of the received signal.
Then, a first order Taylor development in the (t,θr,θe) signal space leads to a linear relation between the variations of the received signal and the variations of the measured travel-time, reception angle and emission angle of each acoustic path after double beamforming.
This paper establishes the mathematical expression of sensitivity kernels and results obtained with synthetic data are shown and discussed.

Keywords: *Helmholtz equation, Beamforming, Born approximation, Green's function, Sensitivity kernel, Travel-time, Reception angle, Emission angle, Waveguide, Parabolic equation, Tomography, Ocean.*

1. INTRODUCTION

Ocean acoustic tomography has been introduced by Munk in 1979. It is based on the same philosophy as the bio-medical tomography: use redundant spatial information given by wave propagation to get slices of the propagation medium. In the ocean the multi-path propagation of acoustic waves is used to get images of the sound speed spatial distribution; itself closely linked to the spatial distribution of seawater temperature.

Classical acoustic tomography uses travel times (TT) of acoustic waves along the different paths. Each travel time provides information on the sound speed along the raypath. Combining the sound speed information gathered on each raypath, it is then possible to estimate the sound speed distribution of the propagation medium [1].

In practice, if travel times of different paths are too close, interferences occur and it is then impossible to separate acoustic arrivals and measure their respective arrival times. To cope with this problem receive arrays combined with array processing have been used. However, even with this processing, it is sometimes hard to separate the first arrivals. That is why recently, double beamforming (DBF) techniques, based on source-receive arrays, have been developed in ocean tomography. Looking at the received signal in terms of travel times, directions-of-arrival and directions-of-departure is most of the time sufficient to separate the different acoustic arrivals. The travel times, but also new observables like angles, can be measured to be used in the tomography process.

Another part of ocean acoustic tomography is to modelize the influence of sound speed variations on the acoustic propagation and consequently on the extracted observables. Originally, using ray theory, only sound speed perturbations located on a raypath were supposed to have an effect on its corresponding arrival. It has been shown that for low frequency signals, an acoustic arrival can be influenced by a celerity perturbation which is not on the raypath [2]. In this configuration, sensitivity kernels can be used to model the effects of sound speed variations on the extracted observables.

In this paper, receive-source arrays and DBF are used to separate paths and to get two additional observables: Direction-of-arrival (DOA) and direction-of-departure (DOD). The associated sensitivity kernels, linking the observables to the sound speed variations, are established and results obtained on synthetic data are shown and discussed.

2. SENSITIVITY KERNELS

1. General Idea

For a given acoustic arrival, sensitivity kernel $K(\boldsymbol{r}')$ links the sound speed distribution variations $\Delta c(\boldsymbol{r}')$ to the variations of the observables measured on the received signal after processing $(\Delta\tau, \Delta\Theta_r \text{ and } \Delta\Theta_e)$. In our case, this relation is linear and given by the following formula:

$$\begin{bmatrix} \Delta\tau \\ \Delta\Theta_r \\ \Delta\Theta_e \end{bmatrix} = \int K(\boldsymbol{r}')\,\Delta c(\boldsymbol{r}')\,dV(\boldsymbol{r}') \qquad (1)$$

The expression of the sensitivity kernel will therefore depends on two different matters: the model taken for the acoustic propagation and the technique used to measure the observables. We first study how the acoustic propagation is modelized and allows to get information on variations of the sound speed distribution. Then we establish the link with the TT, DOA and DOD obtained through DBF.

In the following, the variations are taken between a reference state where variables are indexed by *0*, and a perturbed state where variables are indexed by the letter *p*. Variables representing the variations between the two states are preceded by Δ.

2. The Green's Function

Thanks to first order approximations of fluid mechanic and thermodynamic equations the acoustic propagation is described by the acoustic form of the d'Alembert equation. For harmonic waves, it can be simplified resulting in the Helmholtz equation. The Green's function is the solution of the non-homogenous Helmholtz equation for a punctual source located in $\boldsymbol{r}'$.

$$\left[\nabla^2 + \frac{\omega^2}{c_0^2(\boldsymbol{r})}\right] G_0(\omega, \boldsymbol{r}, \boldsymbol{r}') = \delta(\boldsymbol{r} - \boldsymbol{r}') \tag{2}$$

where ω is the pulsation of the signal, $\boldsymbol{r}$ a point in the propagation medium, $\boldsymbol{r}'$ the source location, $c_0(\boldsymbol{r})$ the sound speed distribution in the reference state at $\boldsymbol{r}$, $G_0(\omega, \boldsymbol{r}, \boldsymbol{r}')$ the Green's function between the source at $\boldsymbol{r}'$ and a point at $\boldsymbol{r}$ and $\delta(\boldsymbol{r} - \boldsymbol{r}')$ the impulsive source at $\boldsymbol{r}'$.

The Green's function can be seen as an impulse response. Therefore, for a distribution of sources $S(\omega, \boldsymbol{r}_e)$ corresponding to the source array, it is possible to write the acoustic field at the receivers thanks to the Green's function. This is made both in the reference and the perturbed state, and the variation of the received signal $\Delta p(t, \boldsymbol{r}_r, \boldsymbol{r}_e)$ can be expressed as a function of the variations of the Green's function $\Delta G(\omega, \boldsymbol{r}_r, \boldsymbol{r}_e)$:

$$\Delta p(t, \boldsymbol{r}_r, \boldsymbol{r}_e) = \frac{1}{2\pi} \int \Delta G(\omega, \boldsymbol{r}_r, \boldsymbol{r}_e) S(\omega, \boldsymbol{r}_e) \exp(i\omega t)\, d\omega \tag{3}$$

3. The First Order Born Approximation

In the ocean, local sound speed variations are usually bellow one percent. To get an expression of the perturbed Green's function, the hypothesis of small variations is made: $\Delta c \ll c_0$ and $\Delta G \ll G_0$.

Under this assumption, the difference between the equation (2) and its equivalent for the perturbed state can be approximated by a first order development in $\Delta c / c_0$ and $\Delta G / G_0$. This result is called first order Born approximation:

$$\left[\nabla^2 + \frac{\omega^2}{c_0^2(\boldsymbol{r})}\right] \Delta G(\omega, \boldsymbol{r}, \boldsymbol{r}') \approx \frac{2\omega^2}{c_0^3(\boldsymbol{r})} G_0(\omega, \boldsymbol{r}, \boldsymbol{r}') \Delta c(\boldsymbol{r}) \tag{4}$$

In this expression it is possible to consider that $\Delta G(\omega, \boldsymbol{r}, \boldsymbol{r}')$ is the solution of the Helmholtz equation of the unperturbed medium for the source distribution

$-2\omega^2/c_0^3(\boldsymbol{r}) \times G_0(\omega,\boldsymbol{r},\boldsymbol{r}')\Delta c(\boldsymbol{r})$. Thus, the variation of the Green's function can be written as a function of the unperturbed Green's function between a source at r_e and a receiver at r_r :

$$\Delta G(\omega,\boldsymbol{r}_r,\boldsymbol{r}_e) \approx \int \frac{-2\omega^2}{c_0^3(\boldsymbol{r}')} G_0(\omega,\boldsymbol{r}_r,\boldsymbol{r}') G_0(\omega,\boldsymbol{r}',\boldsymbol{r}_e)\Delta c(\boldsymbol{r}')\, dV(\boldsymbol{r}') \quad (5)$$

At this step, combining equations 3 and 5, we obtain the link between the sound speed perturbations $\Delta c(\boldsymbol{r}')$ and the received signal variations $\Delta p(t,\boldsymbol{r}_r,\boldsymbol{r}_e)$.

4. Extraction of the Observables

The goal of this part is to extract observables (travel-time, direction-of-arrival and direction-of-departure) using double beamforming (DBF) and link their variations to the received signal variations [3].

Invoking the spatial reciprocity principle, a time delay beamforming (delay and sum), is applied simultaneously on the source and receive arrays leading to a representation of the data with respect to their DOA, DOD and TT. From the recorded waveguide transfer matrix $p(t,\boldsymbol{r}_r,\boldsymbol{r}_e)$depending on the travel times, receiver position and source position, we obtain a new representation $p(t,\theta_r,\theta_e)$ linked to a reference receiver and a reference source (resp. at $\boldsymbol{r}_{r0}$ and $\boldsymbol{r}_{e0}$).

The formulation obtained for the received signal variations is:

$$\Delta p(t,\theta_r,\theta_e) = \frac{1}{2\pi}\int \sum_m \sum_n \Delta P(\omega,\boldsymbol{r}_{rm},\boldsymbol{r}_{en}) \exp\left(i\omega\left[t + T_{rm}(\theta_r) + T_{en}(\theta_e)\right]\right) d\omega \quad (6)$$

where:

$\Delta P(\omega,\boldsymbol{r}_{rm},\boldsymbol{r}_{en})$ is the Fourier transform at the frequency ω of the acoustic perturbation recorded on the receiver $\boldsymbol{r}_{rm}$ for a source $\boldsymbol{r}_{en}$.

$T_{rm}(\theta_r) = \dfrac{(\boldsymbol{r}_{rm} - \boldsymbol{r}_{r0})\sin(\theta_r)}{c_0(\boldsymbol{r}_r)}$ is the delay applied to the mth receiver for a DOA θ_r.

$T_{en}(\theta_e) = \dfrac{(\boldsymbol{r}_{en} - \boldsymbol{r}_{e0})\sin(\theta_e)}{c_0(\boldsymbol{r}_e)}$ is the delay applied to the nth source for a DOD θ_e.

These delay expressions are true only in the case of plane wave and if the sound speed along the source and receive arrays, respectively $c_0(r_e)$and $c_0(r_r)$, does not vary.

After DBF, each maximum corresponds to an acoustic arrival and it is possible to extract its travel time τ, its direction of arrival Θ_r and its direction of departure Θ_e.

In the reference state, partial derivatives are null at the maximum $(\tau_{0,}\Theta_{r0},\Theta_{e0})$:

$$\frac{\partial p_0(\tau_{0,}\Theta_{r0},\Theta_{e0})}{\partial t} = 0 \quad ; \quad \frac{\partial p_0(\tau_{0,}\Theta_{r0},\Theta_{e0})}{\partial \theta_r} = 0 \text{ and } \frac{\partial p_0(\tau_{0,}\Theta_{r0},\Theta_{e0})}{\partial \theta_e} = 0 \quad (7)$$

In the perturbed state, partial derivatives are also null at the maximum $(\tau_{p,}\Theta_{rp},\Theta_{ep})$. In order to introduce the observable perturbations, a first order Taylor development of the perturbed pressure signal is made around $(\tau_{0,}\Theta_{r0},\Theta_{e0})$:

$$\begin{cases} \dfrac{\partial p_p\left(\tau_{p,}\Theta_{rp},\Theta_{ep}\right)}{\partial t} = \dfrac{\partial p_p\left(\tau_{0,}\Theta_{r0},\Theta_{e0}\right)}{\partial t} + \Delta\tau\dfrac{\partial^2 p_p\left(\tau_{0,}\Theta_{r0},\Theta_{e0}\right)}{\partial t^2} + \Delta\Theta_r\dfrac{\partial^2 p_p\left(\tau_{0,}\Theta_{r0},\Theta_{e0}\right)}{\partial\theta_r\partial t} + \Delta\Theta_e\dfrac{\partial^2 p_p\left(\tau_{0,}\Theta_{r0},\Theta_{e0}\right)}{\partial\theta_e\partial t} \\ \dfrac{\partial p_p\left(\tau_{p,}\Theta_{rp},\Theta_{ep}\right)}{\partial\theta_r} = \dfrac{\partial p_p\left(\tau_{0,}\Theta_{r0},\Theta_{e0}\right)}{\partial\theta_r} + \Delta\tau\dfrac{\partial^2 p_p\left(\tau_{0,}\Theta_{r0},\Theta_{e0}\right)}{\partial t\partial\theta_r} + \Delta\Theta_r\dfrac{\partial^2 p_p\left(\tau_{0,}\Theta_{r0},\Theta_{e0}\right)}{\partial\theta_r^{\,2}} + \Delta\Theta_e\dfrac{\partial^2 p_p\left(\tau_{0,}\Theta_{r0},\Theta_{e0}\right)}{\partial\theta_e\partial\theta_r} \\ \dfrac{\partial p_p\left(\tau_{p,}\Theta_{rp},\Theta_{ep}\right)}{\partial\theta_e} = \dfrac{\partial p_p\left(\tau_{0,}\Theta_{r0},\Theta_{e0}\right)}{\partial\theta_e} + \Delta\tau\dfrac{\partial^2 p_p\left(\tau_{0,}\Theta_{r0},\Theta_{e0}\right)}{\partial t\partial\theta_e} + \Delta\Theta_r\dfrac{\partial^2 p_p\left(\tau_{0,}\Theta_{r0},\Theta_{e0}\right)}{\partial\theta_r\partial\theta_e} + \Delta\Theta_e\dfrac{\partial^2 p_p\left(\tau_{0,}\Theta_{r0},\Theta_{e0}\right)}{\partial\theta_e^{\,2}} \end{cases} \quad (8)$$

In order to theoretically inverse the system and get clearer expressions of sensitivity kernels, the cross terms are considered to be null. In practice, the maximal error made on the sensitivity kernels when these terms are neglected is 5%.
The system becomes then three independent differential equations that can be solved independently:

$$\Delta\tau = \frac{\dfrac{-\partial p_p\left(\tau_{0,}\Theta_{r0},\Theta_{e0}\right)}{\partial t}}{\dfrac{\partial^2 p_p\left(\tau_{0,}\Theta_{r0},\Theta_{e0}\right)}{\partial t^2}},\ \Delta\Theta_r = \frac{\dfrac{-\partial p_p\left(\tau_{0,}\Theta_{r0},\Theta_{e0}\right)}{\partial\theta_r}}{\dfrac{\partial^2 p_p\left(\tau_{0,}\Theta_{r0},\Theta_{e0}\right)}{\partial\theta_r^2}} \text{ and } \Delta\Theta_e = \frac{\dfrac{-\partial p_p\left(\tau_{0,}\Theta_{r0},\Theta_{e0}\right)}{\partial\theta_e}}{\dfrac{\partial^2 p_p\left(\tau_{0,}\Theta_{r0},\Theta_{e0}\right)}{\partial\theta_e^2}}. \quad (9)$$

In the equations above, we replace $p_p\left(t,\theta_r,\theta_e\right)$ by $p_0\left(t,\theta_r,\theta_e\right)+\Delta p\left(t,\theta_r,\theta_e\right)$. By using the equation 7, the first order derivatives of $p_0\left(t,\theta_r,\theta_e\right)$ in $\left(\tau_{0,}\Theta_{r0},\Theta_{e0}\right)$ are null. Then, under the assumption of small perturbations, we considered only terms with the lowest perturbation order. This leads to the following relations linking the observables to the signal after DBF:

$$\Delta\tau = \frac{\dfrac{-\partial\Delta p\left(\tau_{0,}\Theta_{r0},\Theta_{e0}\right)}{\partial t}}{\dfrac{\partial^2 p_0\left(\tau_{0,}\Theta_{r0},\Theta_{e0}\right)}{\partial t^2}},\ \Delta\Theta_r = \frac{\dfrac{-\partial\Delta p\left(\tau_{0,}\Theta_{r0},\Theta_{e0}\right)}{\partial\theta_r}}{\dfrac{\partial^2 p_0\left(\tau_{0,}\Theta_{r0},\Theta_{e0}\right)}{\partial\theta_r^2}} \text{ and } \Delta\Theta_e = \frac{\dfrac{-\partial\Delta p\left(\tau_{0,}\Theta_{r0},\Theta_{e0}\right)}{\partial\theta_e}}{\dfrac{\partial^2 p_0\left(\tau_{0,}\Theta_{r0},\Theta_{e0}\right)}{\partial\theta_e^2}}. \quad (10)$$

The combination of the equations 6 and 10 relates the observable perturbations, $\Delta\tau,\Delta\Theta_r$ and $\Delta\Theta_e$, to the received signal variations $\Delta p\left(t,\theta_r,\theta_e\right)$, which represents the signal processing part of the process.

5. Expression of the Sensitivity Kernels

The link between the observable variations and the sound speed variations can be established using successively the equations 3 and 5, which represent the physical model, and the equations 6 and 10, which correspond to the signal processing part.

It comes out the following expressions of the travel-times, directions-of-arrival and directions-of-departure sensitivity kernels, respectively written K_{TT},K_{DOA} and K_{DOD}:

$$K_{TT}\left(\boldsymbol{r}'\right) = \frac{1}{2\pi}\int\sum_m\sum_n \frac{i\omega}{\dfrac{\partial^2 p_0\left(\tau_{0,}\Theta_{r0},\Theta_{e0}\right)}{\partial t^2}} Q\left(\omega,\boldsymbol{r_{rm}},\boldsymbol{r_{en}},\boldsymbol{r}'\right)\exp\left(i\omega\left[\tau_0+T_{rm}\left(\Theta_{r0}\right)+T_{en}\left(\Theta_{e0}\right)\right]\right)d\omega \quad (11)$$

$$K_{DOD}(\boldsymbol{r}') = \frac{1}{2\pi}\int \sum_m \sum_n \frac{i\omega(\boldsymbol{r}_{en}-\boldsymbol{r}_{e0})\cos(\Theta_{e0})}{c_0(\boldsymbol{r}_e)\dfrac{\partial^2 p_0(\tau_{0,}\Theta_{r0},\Theta_{e0})}{\partial\Theta_e^2}} Q(\omega,\boldsymbol{r}_{rm},\boldsymbol{r}_{en},\boldsymbol{r}')\exp\left(i\omega\left[\tau_0 + T_{rm}(\Theta_{r0}) + T_{en}(\Theta_{e0})\right]\right)d\omega \quad (12)$$

$$K_{DOA}(\boldsymbol{r}') = \frac{1}{2\pi}\int \sum_m \sum_n \frac{i\omega(\boldsymbol{r}_{rm}-\boldsymbol{r}_{r0})\cos(\Theta_{r0})}{c_0(\boldsymbol{r}_r)\dfrac{\partial^2 p_0(\tau_{0,}\Theta_{r0},\Theta_{e0})}{\partial\Theta_r^2}} Q(\omega,\boldsymbol{r}_{rm},\boldsymbol{r}_{en},\boldsymbol{r}')\exp\left(i\omega\left[\tau_0 + T_{rm}(\Theta_{r0}) + T_{en}(\Theta_{e0})\right]\right)d\omega \quad (13)$$

where

$$Q(\omega,\boldsymbol{r}_{rm},\boldsymbol{r}_{en},\boldsymbol{r}') = \frac{2\omega^2}{c_0^3(\boldsymbol{r}')}G_0(\omega,\boldsymbol{r}_{rm},\boldsymbol{r}')G_0(\omega,\boldsymbol{r}',\boldsymbol{r}_{en})S(\omega,\boldsymbol{r}_{en})$$

It can be noticed that the term $Q(\omega,\boldsymbol{r}_{rm},\boldsymbol{r}_{en},\boldsymbol{r}')$ is common to all the sensitivity kernels. This term can be seen like the influence of a diffracting point $\boldsymbol{r}'$.

The sensitivity kernel is also depending on the inverse of the bending of the arrival. TT sensitivity kernel depends on the inverse of the bending in time $\left[\partial^2 p_0(\tau_{0,}\Theta_{r0},\Theta_{e0})/\partial t^2\right]^{-1}$; DOD sensitivity kernel depends on the inverse of the bending in emission angle $\left[\partial^2 p_0(\tau_{0,}\Theta_{r0},\Theta_{e0})/\partial\Theta_e^2\right]^{-1}$; and DOA sensitivity kernel depends on the inverse of the bending in reception angle $\left[\partial^2 p_0(\tau_{0,}\Theta_{r0},\Theta_{e0})/\partial\Theta_r^2\right]^{-1}$.

Another similarity can be noticed between these sensitivity kernels: the partial derivatives of the signal phase. For TT sensitivity kernels this term is represented by $i\omega$. For DOD and DOA sensitivity kernels these terms are respectively $i\omega(\boldsymbol{r}_{en}-\boldsymbol{r}_{e0})\cos(\Theta_{e0})/c_0(\boldsymbol{r}_e)$ and $i\omega(\boldsymbol{r}_{rm}-\boldsymbol{r}_{r0})\cos(\Theta_{r0})/c_0(\boldsymbol{r}_r)$.

Note that, in the case of the DOD (resp. DOA), there is an antisymmetry of the phase partial derivatives depending on the position of the considered source (resp. receiver) regarding the reference of the source array (resp. receiver array). This means that the influence of a perturbation will have opposite consequences whether it is located above or under the array reference.

3. RESULTS ON SYNTHETIC DATA

Examples of sensitivity kernels are computed thanks to simulations in an unbounded medium. Two vertical arrays of 30 m, made out of 61 hydrophones evenly spaced, are separated horizontally by 2000 m, in a propagation medium with a uniform sound speed of 1500 m/s.

The medium is parameterized by a cartesian system of coordinates where *r* is the range, *y* is the lateral dimension and *z* the depth (oriented downward). The plan containing the two arrays is *y=0*, the origin in range is taken at the source array and the *z* origin has been taken such that the middles of the arrays are located at 50 m.

The Green's function in unbounded medium is used to model the signal propagation between two points $\boldsymbol{r}$ and $\boldsymbol{r}'$ [4]:

$$G(\omega,\mathbf{r},\mathbf{r}') = \frac{\exp\left(i\frac{\omega}{c_0}|\mathbf{r}-\mathbf{r}'|\right)}{4\pi|\mathbf{r}-\mathbf{r}'|} \qquad (14)$$

This model generates the reference signal needed for the computation of the sensitivity kernels. The transmitted signal is a 3KHz central frequency, with a 2KHz bandwidth. At the end, one time series is obtained for every couple transmitter/receiver: $p(t,\mathbf{r}_r,\mathbf{r}_e)$.

Note that in the implementation, all the terms of the Hessian matrix has been taken into account. The differential system inversion has been done numerically.

Figures 1 and 2 show respectively the TT-sensitivity kernel in $s.(m.s^{-1}.m^3)^{-1}$ and the DOD-sensitivity kernels in $deg.(m.s^{-1}.m^3)^{-1}$. The DOA-sensitivity kernel is not shown here since it is the exact symmetry of the DOD sensitivity kernels with respect to the plan *r = 1000 m*.

Figure 1 shows that TT sensitivity kernels have three plans of symmetry: *r = 1000 m, y = 0 m* and *z = 50 m*. The area of maximal sensitivity is located in the vicinity of the raypath.

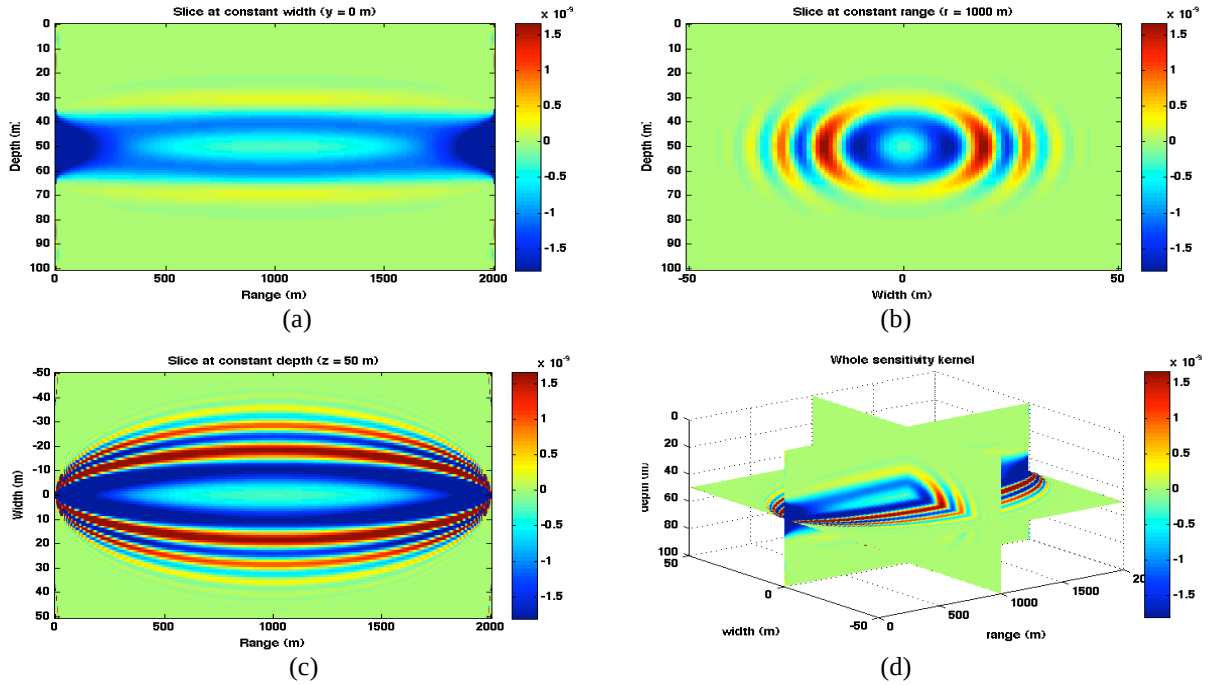

Fig 1: The figures a, b, and c represent slices of the TT sensitivity kernel respectively at constant lateral dimension, constant range and constant depth. The figure d is the 3D combination of the 3 previous ones. The TT sensitivity kernel is in $s.(m.s^{-1}.m^3)^{-1}$.

DOD sensitivity kernel has one antisymmetry plan: *z = 50 m* (Fig. 2). The sensitivity is null on this plan which means that sound speed variations located at 50 m depth do not change the emission angle (Fig. 2-c). Areas of strong opposite sensitivity are found on each side of the raypath and fade away as we get far from the raypath.

We can note that TT and DOD sensitivity kernels contain complementary information. On the raypath the DOD sensitivity kernel is null whereas the TT sensitivity kernel is not. Close to the raypath, DOD sensitivity kernel allows to make the difference between perturbations located above or bellow the raypath which is not the case with TT sensitivity kernel.

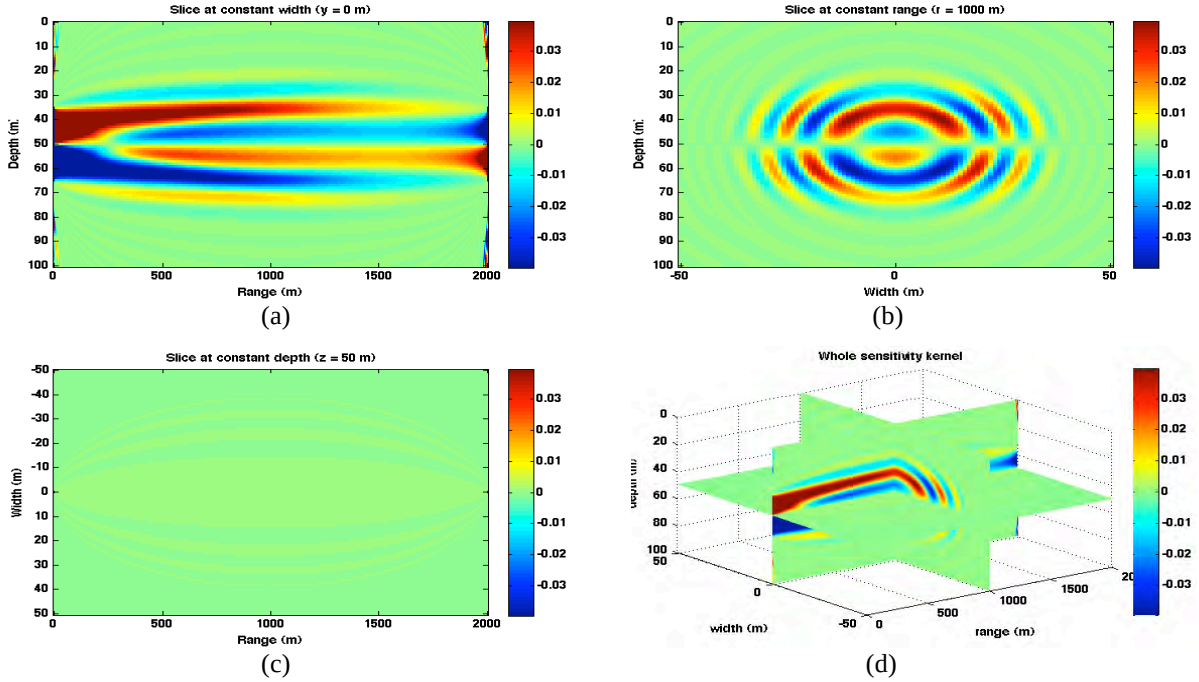

Fig 2: The figures a, b, and c represent slices of the DOD sensitivity kernel respectively at constant lateral dimension, constant range and constant depth. The figure d is the 3D combination of the 3 previous ones. The DOD sensitivity kernel is in deg.$(m.s^{-1}.m^3)^{-1}$.

4. CONCLUSION AND PERSPECTIVES

It has been demonstrated that directions-of-arrivals and directions-of-departure can be used jointly with travel times, as observables, to build sensitivity kernels. Such sensitivity kernels have been shown for unbounded medium synthetic data. The next steps will consist in establishing them in waveguides and use them to solve the inverse problem: get an image of sound speed variations from observables variations.

5. REFERENCES

[1] **Munk, W. and Wunsch, C.**, Ocean acoustic tomography: a scheme for large scale monitoring, Deep Sea Research Part A. Oceanographic Research Papers, Elsevier, 26, 123-161 1979

[2] **Skarsoulis, E. K. and Cornuelle, B. D.**, Travel-time sensitivity kernels in ocean acoustic tomography, Journal of the Acoustical Society of America, 116, 228-238, 2004.

[3] **Iturbe, I. ; Roux, P. ; Nicolas, B. ; Virieux, J. and Mars, J. I.**, Shallow-water acoustic tomography performed from a double-beamforming algorithm: simulation results, IEEE Journal of, IEEE, 34, 140-149, 2009.

[4] **Jensen, F.B.**, Computational ocean acoustics, R. T. Beyer, AIP series, 1994.